Spectrochimica Acta Part A: Molecular and Biomolecular Spectroscopy 244 (2021) 118830

Contents lists available at ScienceDirect

Spectrochimica Acta Part A: Molecular and Biomolecular Spectroscopy

journal homepage: www.elsevier.com/locate/saa

A fluorescent sensor for selective detection of hypochlorite and its application in *Arabidopsis thaliana*

Zi-Xuan Zeng [a,1], Jin Gu [a,1], Ya-Ni Liu [a], Dong-Dong Li [b], Yu-Shun Yang [a,*], Bao-Zhong Wang [a,*], Hai-Liang Zhu [a,*]

[a] State Key Laboratory of Pharmaceutical Biotechnology, School of Life Sciences, Nanjing University, Nanjing 210023, China
[b] College of Chemical Engineering, Nanjing Forestry University, 159 Longpan Road, Nanjing 210037, China

ARTICLE INFO

Article history:
Received 8 July 2020
Received in revised form 4 August 2020
Accepted 9 August 2020
Available online 15 August 2020

Keywords:
Hypochlorite detection
Fluorescent sensor
Biological imaging
Plant tissue
Nitrone-involved mechanism

ABSTRACT

Hypochlorite, as one of reactive oxygen species, has drawn much attention due to its essential roles in special biological events and disorders. The exogenous hypochlorite remains a risk for human, animals and plants. In this work, a novel water soluble quinolin-containing nitrone derivative T has been developed for fluorometric sensing hypochlorite. The response mechanism of T towards ClO^- was reported for the first time. In comparison with the reported sensors for ClO^-, the sensor **T** in this work exhibited advantages including high selectivity (80 fold over other analytes), rapid response (within 5 s) and lipid-water distribution transformation (LogP from 2.979 to 6.131). Further biological applications suggested that **T** was capable of monitoring both exogenous and endogenous ClO^- in living cells. The imaging in *Arabidopsis thaliana* indicated that the absorption and transmission of ClO^- in plant could be monitored by this sensor through the chlorine-related mechanism. This work might raise referable information for further investigations in the physiological and pathological events in both tumor and plants.

1. Introduction

Since the fluorescent sensors guided the prosperity in chemical biology in the recent decade [1,2], the concomitant sensing approaches have started to challenge the traditional analytical methods including electrochemistry [3], Raman spectroscopy [4], colorimetry [5], titrimetry [6], chromatography [7], and so on. Generally, the advantages of the fluorescent implements include simple preparation of samples, convenient technical procedures, and of course the most important properties such as high sensitivity, high selectivity and good biocompatibility [8,9]. To date, many practical fluorescent sensors have been exploited for the detection of various chemical species via lots of mechanisms [10].

Among the chemical species, reactive oxygen species (ROS) act as the significant indicators of physiological and pathological procedures [11,12], thus have accordingly been utilized in diagnostic and therapeutic applications [13–15]. In particular, as one of the ROS, hypochlorite (ClO^-) has drawn much attention due to its essential roles in special biological events such as the prevention of microorganism invasion [16]. In organisms, hypochlorite is commonly synthesized from hydrogen peroxide and chloride ions in a biosystem catalyzed by myeloperoxidase (MPO) [17]. It can cause the damage of DNA, RNA, fatty acids, cholesterol, and proteins [18]. Therefore, the hypochlorite level is tightly associated with disorders and diseases such as atherosclerosis, arthritis, and cancers [19]. The exogenous hypochlorite mainly came from the disinfection agent in drinking water treatment, which remains a risk for human, animals and plants [20,21]. Thus the detection of hypochlorite could not only reveal the indistinct mechanism of disease occurrence and development, but also hint new therapeutic schedules via ROS production [22].

A certain number of fluorescent sensors have been developed for monitoring hypochlorite. Begining at about 2010 [23] and booming from approximate 2016 [24], the researches on sensing hypochlorite have involved lots of chromophores such as Nile Blue, phenothiazines, fluorescein, benzothiazole, 1,8-naphthalimide, BODIPY and Iridium complexes as well as various mechanisms including oxidation, deprotection, breaking double bond and logical gate [25–44]. To overcome the reported limitations such as narrow practical pH range, complicated synthesis, poor water-solubility and low selectivity, novel fluorescent sensors with new mechanisms are still in urgent need.

In this work, a novel water soluble quinolin-containing nitrone derivative **T** has been developed for fluorometric sensing hypochlorite (Fig. 1). The response mechanism of **T** towards ClO^- was reported for the first time. These fluorescent sensors seemed unique among the recent hypochlorite sensing reports [25–44]. With practical optical and recognizing performances, the sensor was further applied to monitor the ClO^- level in cancer cells and *Arabidopsis thaliana*.

* Corresponding authors.
E-mail addresses: ys_yang@nju.edu.cn (Y.-S. Yang), wbz@nju.edu.cn (B.-Z. Wang), zhuhl@nju.edu.cn (H.-L. Zhu).
[1]Both authors contributed equally to the work.

https://doi.org/10.1016/j.saa.2020.118830
1386-1425/

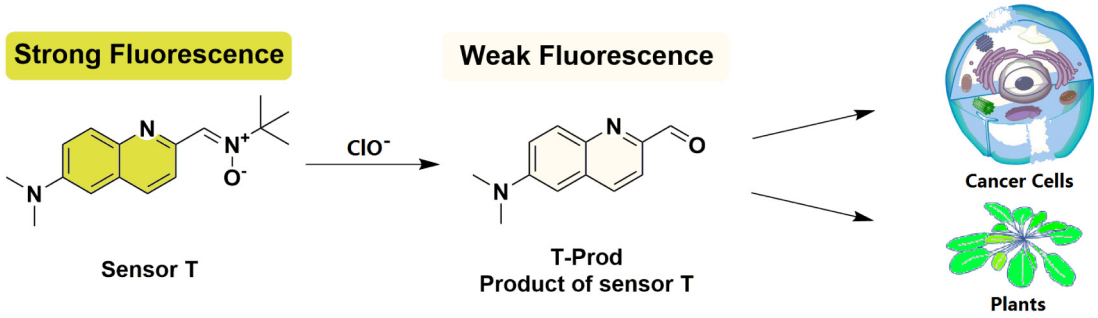

Fig. 1. Illustration of the fluorescent sensor **T** for monitoring hypochlorite.

2. Experimental

2.1. The experimental materials and equipment

All chemicals purchased were used as received without further purification. The products were purified by 300–400 mesh chromatography silica gel. All NMR data of the compounds were measured by Bruker (Rhenistetten-Forchheim, Germany) AM 600 MHz, collected in Chloroform-*d* or DMSO-d_6 and dealt with MestReNova software (Mestrelab Research, Santiago de Compostela, Spain). Mass spectra were acquired from an Agilent 6540 UHD Accurate Mass Q-TOF LC/MS (Agilent Technologies Inc., California, USA). UV–vis spectra were detected on Shimadzu UV-2550 spectrometer (Shimadzu Corp., Tokyo, Japan). The fluorescence intensity detection was accomplished on Hitachi Fluorescence Spectrophotometer F-7000 (Hitachi Ltd., Tokyo, Japan). pH calibration was conducted by pH meter of PHS-25. Cell viability experiments were carried out using MTT method. Bioimaging experiment was presented on Leica TCS SP8-MaiTai M double-photon confocal fluorescent microscope (Leica Camera AG, Weztlar, Germany).

2.2. Determination of LogP values

Aqueous sodium chloride (0.9% w/v) and organic (*n*-octanol) phases were saturated for 1 week. The tested compounds were dissolved at a final concentration of 300 μM in the aqueous phase. An equal volume of saturated *n*-octanol was added and the solutions mixed for 30 min under 45 rpm. Samples were centrifuged (1500*g*, 10 min) and the tested compound content of the organic and aqueous phases was determined by UV absorbance at 280 nm. The LogP values were then defined as the logarithmic ratio of test compound concentrations in the organic and aqueous phases.

2.3. Synthesis of the sensors

The general synthesis route of the sensor **T** and the intermediate **T-Prod** (also the detecting product) was illustrated in Fig. 2. 4-*N*,*N*-Dimethylamino aniline (Compound **1**, 5 g, 36.7 mmol, 1.0 equiv) was added into a solution of HCl (6 M, 66 mL). Then crotonaldehyde (6.0 mL, 73.5 mmol, 2 equiv) was added into the mixture and stirred at room temperature for 1 h. Afterwards, toluene (35 mL) was added and the reaction was kept refluxing at 115 °C overnight. After cooling down to room temperature, the toluene layer was removed. The saturated sodium hydroxide solution was added to neutralize the aqueous layer. The solution was extracted with CH_2Cl_2, washed with saturated sodium chloride solution for three times, dried over anhydrous sodium sulfate, filtered and concentrated by evaporation under reduced pressure. The crude product was purified by column chromatography on silica gel (PE: EA = 4:1 v/v) to gain intermediate **2** as a sand-brown solid (3.6 g, 70%). Subsequently, selenium dioxide (2.8 g, 25.1 mmol, 1.3 equiv) was dissolved. The solution was heated at 80 °C for 30 min. Intermediate **2** (3.5 g, 19.2 mmol, 1 equiv) was then added and the mixture was refluxed at 80 °C for 4 h. After being cooled down to room temperature, the mixture was filtered and the residue was washed three times by CH_2Cl_2. The filtrate was concentrated by evaporation under reduced pressure to obtain crude product which was purified by column chromatography on silica gel (PE: EA = 6:1 v/v). The acquired quinoline aldehyde **T-Prod** (also the detecting product) was yellow solid (1.52 g, 40%).

The intermediate **T-Prod** (200 mg, 1.0 mmol) and pyrrolidine (85.44 mg, 1.2 mmol) were dissolved in CH_2Cl_2 (10 mL) for 10 min. *N*-(*tert*-Butyl) hydroxylamine hydrochloride (125.6 mg, 1 mmol) was added into the solution. The mixture was stirred at room temperature for 4 h. After the completion of the reaction confirmed by TLC, the solvent was condensed by evaporation and was then purified by thin-layer chromatography (PE: EA = 1:2, v/v) to gain the sensor **T**, (*Z*)-*N*-*tert*-butyl-1-(6-(dimethylamino)quinolin-2-yl)methanimine oxide as tawny solid (35 mg). Yield: 17.5%. ^{1}H NMR (600 MHz, Chloroform-*d*) δ 9.15 (d, J = 8.8 Hz, 1H), 8.02 (d, J = 8.8 Hz, 1H), 7.90 (d, J = 9.2 Hz, 1H), 7.37 (d, J = 12.0 Hz, 1H), 6.79 (s, 1H), 3.11 (s, 6H), 1.66 (s, 9H). ^{13}C NMR (151 MHz, DMSO-d_6) δ 152.02, 146.63, 141.01, 132.95, 127.98, 127.45, 121.21, 120.52, 100.21, 29.16, 23.69.

3. Results and discussion

3.1. Synthesis of the sensor

The sensor **T** and the intermediates were synthesized as shown in Fig. 2 and confirmed by satisfactory spectroscopic data (^{1}H NMR, ^{13}C NMR, HRMS, Figs. S5–10, SI).

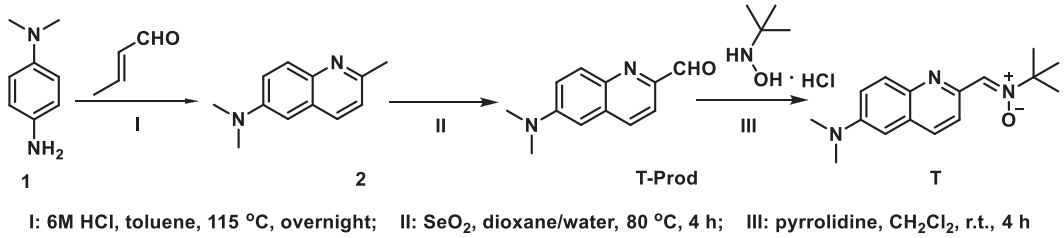

Fig. 2. General synthesis route of the sensor **T** and the intermediates.

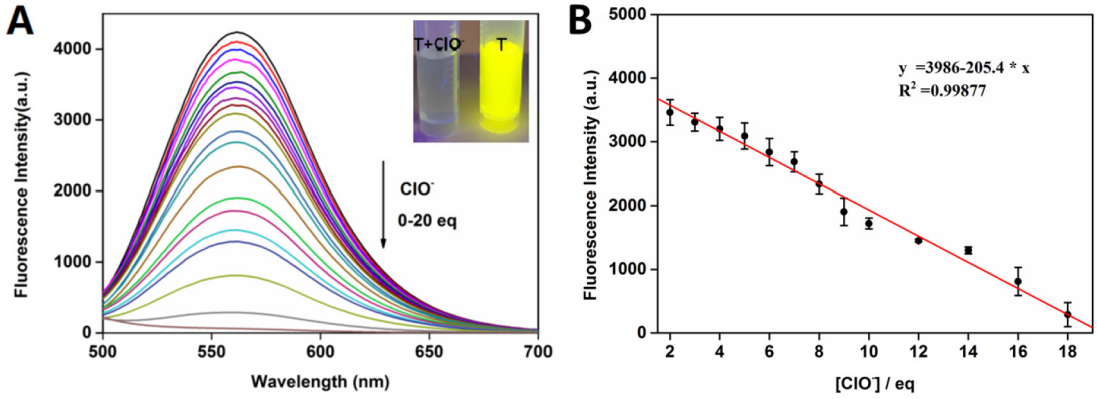

Fig. 3. (A) The fluorescence spectra of the sensor **T** (10 μM) in PBS buffer (10 mM, pH 7.4, 1% DMSO) after treatment with hypochlorite (0–20 equiv.) for 5 min; (B) The linear relationship between the fluorescence intensity and the concentration of hypochlorite (0–20 equiv.) in PBS buffer (10 mM, pH 7.4, 1% DMSO) for 5 min.

*3.2. Fluorescent analytical performance of sensor **T***

Initially, we evaluated the fluorescent properties of the sensor **T** in buffered aqueous media (physiological pH 7.4, 10 mM PBS, 1% DMSO as a co-solvent). With the addition of ClO^-, the absorption peak exhibited a blue-shift and the color changed to transparency under naked-eye observation instantaneously (Fig. S1, SI). As we expected, under the excitation wavelength of 460 nm, the free sensor **T** presented an obvious luminous chartreuse fluorescence emission peak at 561 nm, whereas with the addition of hypochlorite, the fluorescence was quenched immediately (Fig. 3). With the increasing hypochlorite concentration, the fluorescence intensity of the systems decreased with a high ratio up to 80-fold reduction. The fluorescent response of **T** towards ClO^- was calculated to cover a linear range from 1×10^{-7} to 2×10^{-4} M, according to linear formula: $y = 3986–205.4 \times x$. The detection limit was calculated as 0.47 μM.

Besides, we checked two important parameters for ROS sensors, pH and response time. In the pH range of 3–12, the sensor **T** showed a constant fluorescence intensity within pH 7–12 while the detecting system of **T** and ClO^- exhibited no fluorescence within pH 3–10 (Fig. S2, SI). Therefore the workable range of **T** was set as pH 7–10, which could cover most of the physiological environments for ROS generation. On the other hand, a time scan (Fig. S3, SI) suggested that the detecting process completed in a very short moment (<5 s), which was extremely suitable for monitoring the rapidly changing ROS level.

3.3. Selectivity and anti-interference ability

The selectivity and anti-interference ability of the sensor **T** were both evaluated (Fig. 4). A variety of competing analytes including ROS, anions and cations were used independently or together with ClO^-. The concentration of the sensor was 10 μM, and the analytes were all set as 200 μM. The data were presented as the ratios of the fluorescence intensity of **T** before (F_0) and after (F_1) the addition of ClO^-. As shown in Fig. 4A, no remarkable fluorescence variation was found in the presence of the other analytes including ions, amino acids and macromolecules (HSA: Human Serum Albumin; BSA: Bovine Serum Albumin). Only ClO^- could quench the fluorescence. Meanwhile, as shown in Fig. 4B, during the incubation of the involved analytes together with ClO^-, the interference on the detecting system was not obvious. Therefore, in the complex intracellular environment, **T** might be a selective sensor with a reliable detecting performance.

3.4. The reaction mechanism and characteristic

As we claimed in the Introduction, the response mechanism of **T** was achieved via the departure of the new reported nitrone recognizing group for hypochlorite sensing (Fig. 5). After comparing the HRMS and ^1H NMR spectra of **T** and **T-Prod**, we confirmed the detecting product of this system (Figs. S5, S7, S8, S10). Being incubated with ClO^-, the nitrone moiety was transferred into the aldehyde, which led to the

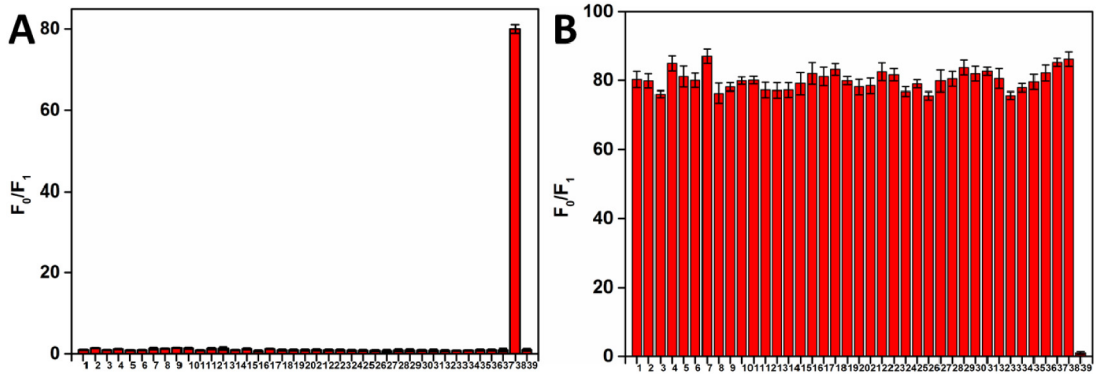

Fig. 4. The ratios of the fluorescence intensity at 561 nm of **T** before (F_0) and after (F_1) the addition of ClO^- in PBS buffer (10 mM, pH 7.4, 1% DMSO). (A) Independent analytes and (B) the coexistence systems with ClO^-: (1) Mn^{2+}; (2) Br^-; (3) K^+; (4) Ni^{2+}; (5) Mg^{2+}; (6) Al^{3+}; (7) I^-; (8) Zn^{2+}; (9) Co^{2+}; (10) Fe^{3+}; (11) SCN^-; (12) HCO_3^-; (13) HSO_4^-; (14) $S_2O_8^-$; (15) H_2O_2; (16) KO_2; (17) Leu; (18) Hcy; (19) Arg; (20) His; (21) Met; (22) Gln; (23) Gly; (24) Ala; (25)Asp; (26) Thr; (27) Ile; (28) Trp; (29) Ser; (30) Glu; (31) Cys; (32) Hsp; (33) GSH; (34) GSH; (35) Val; (36) HSA; (37) BSA; (38) ClO^-; (39) Sensor **T** only.

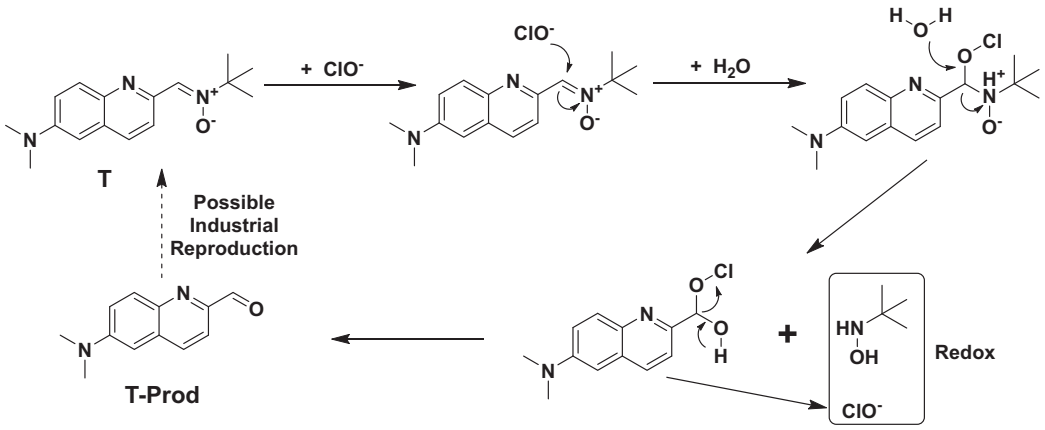

Fig. 5. The illustration of the sensing mechanism of the sensor **T** towards hypochlorite.

change of the chartreuse fluorescence into a faint orange one (even no obvious signal if the excitation of 460 nm was not adjusted). It was a pity that it seemed difficult for us to capture the intermediate during the response due to the transitory process, but we could still be hinted from the rare report on this reaction that the chlorine of hypochlorite participated in the sensing procedure [45]. Instead of experiencing a catalysis-like procedure, the redox pair of hydroxylamine and ClO^- limited the regeneration of ClO^-, thus promoted the equilibrium of the detecting reaction. Moreover, we believed that the sensor **T** experienced a transformation in the preference of lipid-water distribution during the detection. The logP (a model for evaluating oil-water partition coefficient) values of **T** and **T-Prod** were calculated as 2.979 and 6.131 (both around the 2–5 range of Lipinski's "Rule of Five" for drugs), respectively. This result suggested that the sensor itself, as a salt-like compound, was more suitable for delivery, while the detecting product, as an amphiphilic molecule, was more favorable for the intracellular imaging.

3.5. Biological imaging

Before the biological imaging, the cytotoxicity of the sensor **T** was evaluated upon MCF-7 (human breast adenocarcinoma cell line) and HEK293T (human embryonic kidney epithelial cell line) cells by using MTT method. As shown in Fig. S4 in SI, after being incubated with the

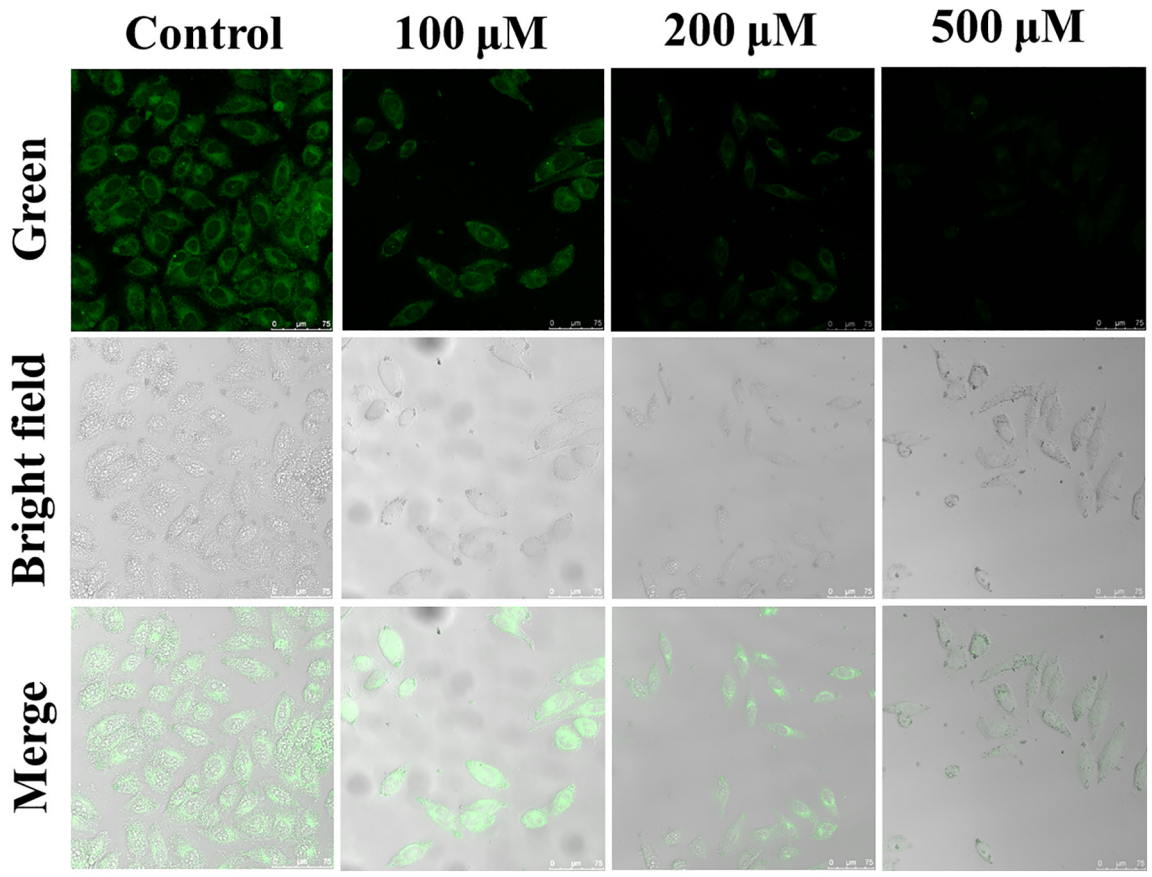

Fig. 6. The confocol images of MCF-7 cells incubated with **T** in different conditions. The concentrations of ClO- were set as 0, 100, 200, 500 μM, respectively. After the incubation with ClO^- for 10 min, a further incubation with 10 μM **T** for 10 min was conducted for each group. The temperature was set as 37 °C. Green channel: collected at 500–600 nm, $\lambda_{ex} = 460$ nm. Scale bar: 75 μm.

sensor **T** (0.1–100 μM) for 24 h, the studied cells maintained a high survival rate over 75%.

Based on the above results, we used **T** to monitor exogenous and endogenous ClO^- in living MCF-7 cells under the fluorescent confocal microscope. As shown in Fig. 6, with the addition of gradient concentrations (0, 100, 200, 500 μM) of ClO^-, the fluorescence of the system remarkably decreased along with the increase of ClO^- concentration.

Furthermore, we studied whether **T** could monitor the endogenously-produced ClO^- in living cells. For the endogenous ClO^-, a typical pair of 1.0 μg/mL lipopolysaccharide (LPS) and 1.0 μg/mL phorbol myristate acetate (PMA) was used as the stimulator, whereas 200 μM 4-azidobenzohydrazide (ABH, a well-known inhibitor of MPO) was used as the blocker [19]. As shown in Fig. 7, the addition of ABH could maintain the fluorescence, whereas the incubation of the LPS/PMA pair could cause an obvious fluorescence decrease in the green channel. A further group containing the LPS/PMA pair together with ABH exhibited no obvious decrease of the fluorescence, which was more close to the control group. The results above indicated that the sensor **T** was capable of monitoring both exogenous and endogenous ClO^- in living cells.

We have demonstrated in the introduction that ClO^- could also affect the plant physiology. In this work, we applied the sensor **T** into the ClO^- detection in both the wild type (WT) and chlorate resistant 1-mutant (CHL, a mutant strain which cannot absorb chlorate) *Arabidopsis thaliana*. Thus we could track the absorption and transmission of ClO^- in this model plant, as well as conversely evidence the participation of chlorine in the response mechanism. As shown in Fig. 8, in the WT group, the absorption of ClO^- within the region near root tip (slightlt behind the tip because the tip was relatively dense) caused an initial enrichment of ClO^-, which could be monitored by the sensor **T** through a decrease of the green fluorescence. The absorbed ClO^- came up along the catheter, therefore the decrease of fluorescence could be observed also in the central catheter region. When it came to the catheter top, the decrease of fluorescence seemed less obvious, which indicated the transformation of ClO^- into other species. However, in the CHL group, the absorption of chlorine was blocked from the very beginning, thus the green fluorescence was not affected in all the investigated regions. Since the major difference of the two groups was the absorption of chlorine, we could infer that the response mechanism was associated with chlorine. Moreover, **T** could be used to monitor ClO^- during specific events in plant physiology.

4. Conclusion

In summary, a novel water soluble quinolin-containing nitrone derivative **T** has been developed for fluorometric sensing hypochlorite. The response mechanism of T towards ClO^- was reported for the first time. In comparison with the reported sensors for ClO^- (Table S1, SI), the sensor **T** in this work exhibited advantages including high selectivity (80 fold over other analytes), rapid response (within 5 s) and lipid-water distribution transformation (LogP from 2.979 to 6.131). The biological application of the sensor **T** was further performed in cancer cells and *Arabidopsis thaliana*. The results indicated that **T** was capable of monitoring both exogenous and endogenous ClO^- in living cells. Moreover, the absorption and transmission of ClO^- in plant could be monitored by this sensor through the chlorine-related mechanism.

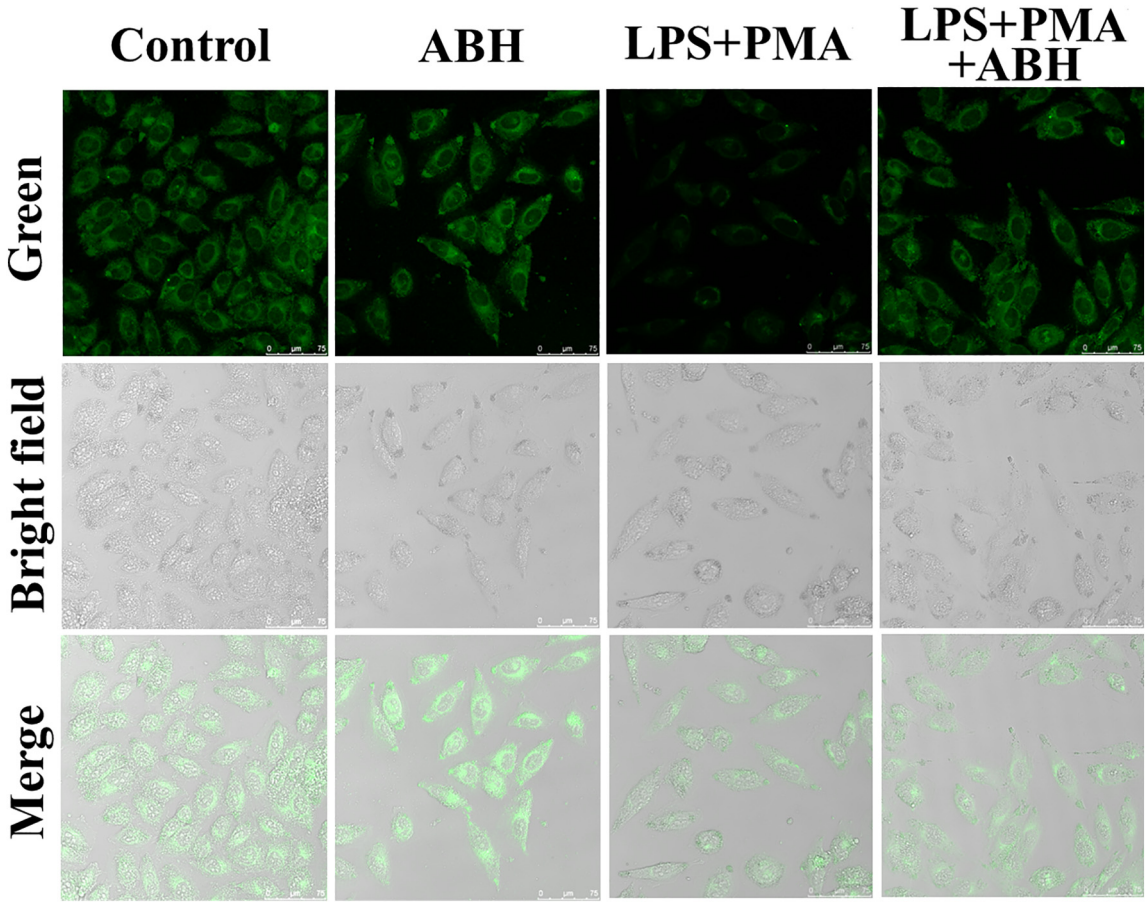

Fig. 7. The confocol images of MCF-7 cells incubated with **T** in different conditions. The concentration of the LPS/PMA pair was set as 1.0 μg/mL each, and that of ABH was set as 200 μM. After the incubation with corresponding agents above for 30 min, a further incubation with 10 μM **T** for 10 min was conducted for each group. The temperature was set as 37 °C. Green channel: collected at 500–600 nm, $\lambda_{ex} = 460$ nm. Scale bar: 75 μm.

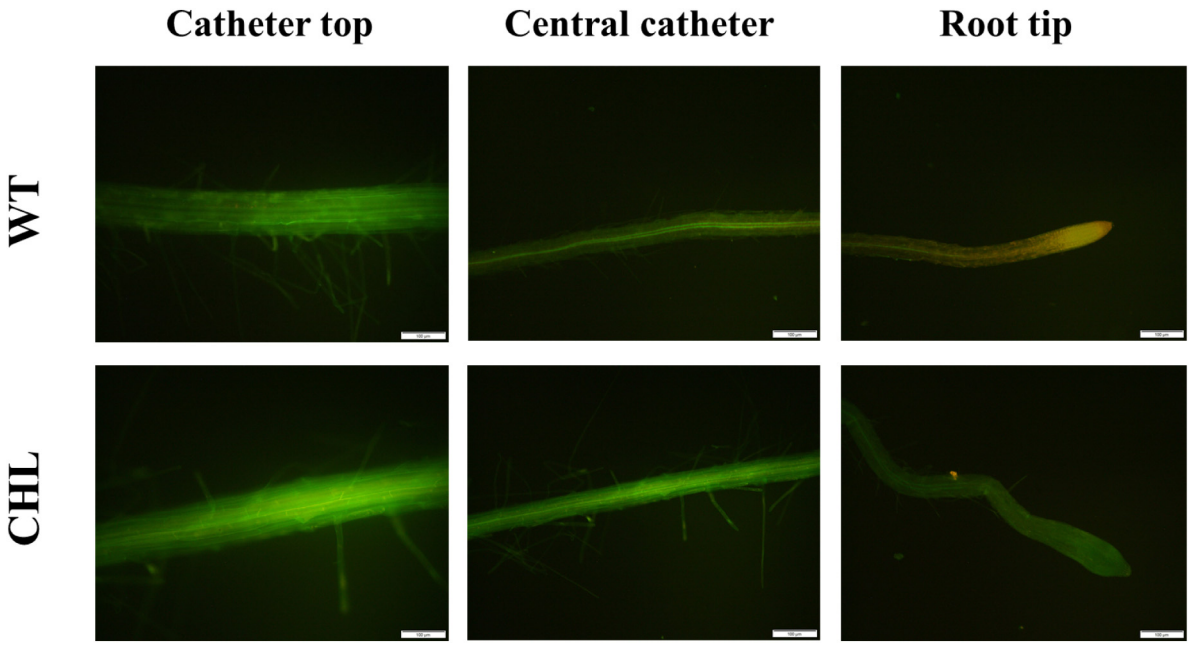

Fig. 8. The confocol images of *Arabidopsis thaliana* incubated with **T** at 25 °C (room temperature). Both the wild type and the chlorate resistant 1-mutant one were involved with the catheter top, central catheter and root tip regions studied. The incubation condition was set as 100 μM ClO^- (30 min, room temperature) and 10 μM **T** (10 min, room temperature). λ_{ex} = 460 nm. Scale bar: 100 μm.

This work might raise referable information for further investigations in the physiological and pathological events in both tumor and plants.

CRediT authorship contribution statement

Zi-Xuan Zeng: Methodology, Formal analysis. **Jin Gu:** Validation, Visualization. **Ya-Ni Liu:** Writing - original draft, Validation. **Dong-Dong Li:** Writing - review & editing. **Yu-Shun Yang:** Conceptualization, Writing - review & editing, Project administration. **Bao-Zhong Wang:** Supervision. **Hai-Liang Zhu:** Funding acquisition.

Declaration of competing interest

All authors declare that there are no conflicts of interest.

Acknowledgments

This work is supported by the Natural Science Research of Jiangsu Higher Education Institutions of China (No. 18KJB350004), and the Project for Young Teachers of Nanjing Forestry University, China (No. CX2017005). Dr. H.L. Zhu thanks for the support of Lianyungang talent project.

Appendix A. Supplementary data

Supplementary data to this article can be found online at https://doi.org/10.1016/j.saa.2020.118830.

References

[1] A.P. de Silva, H.Q.N. Gunaratne, T. Gunnlaugsson, A.J.M. Huxley, C.P. McCoy, J.T. Rademacher, T.E. Rice, Signaling recognition events with fluorescent sensors and switches, Chem. Rev. 97 (1997) 1515–1566.
[2] J.S. Wu, W.M. Liu, J.C. Ge, H.Y. Zhang, P.F. Wang, New sensing mechanisms for design of fluorescent chemosensors emerging in recent years, Chem. Soc. Rev. 40 (2011) 3483–3495.
[3] M.M. Hossain, E.H.B. Anari, L. Aldous, Electrochemistry of chloride in ambient room temperature ionic liquids: formation of oxychloride species, Electrochem. Commun. 34 (2013) 331–334.
[4] A. Draksharapu, D. Angelone, M.G. Quesne, S.K. Padamati, L. Gomez, R. Hage, M. Costas, W.R. Browne, S.P. de Visser, Identification and spectroscopic characterization of nonheme iron(III) hypochlorite intermediates, Angew. Chem. Int. Ed. 54 (2015) 4357–4361.
[5] Z.N. Wei, H.Q. Li, S.B. Liu, W. Wang, H.L. Chen, L.H. Xiao, C.L. Ren, X.G. Chen, Carbon dots as fluorescent/colorimetric probes for real-time detection of hypochlorite and ascorbic acid in cells and body fluid, Anal. Chem. 91 (2019) 15477–15483.
[6] S.B. Jonnalagadda, P. Gengan, Titrimetric and photometric methods for determination of hypochlorite in commercial bleaches, J. Environ. Sci. Heal. A 45 (2010) 917–922.
[7] J.P.E. Spencer, M. Whiteman, A. Jenner, B. Halliwell, Nitrite-induced deamination and hypochlorite-induced oxidation of DNA in intact human respiratory tract epithelial cells, Free Radical Bio. Med. 28 (2000) 1039–1050.
[8] C.W. Lin, S.M. Bachilo, Y. Zheng, U. Tsedev, S.N. Huang, R.B. Weisman, A.M. Belcher, Creating fluorescent quantum defects in carbon nanotubes using hypochlorite and light, Nat. Commun. 10 (2019) Article Number 2874.
[9] X.J. He, H. Chen, C.C. Xu, J.Y. Fan, W. Xu, Y.H. Li, H. Deng, J.L. Shen, Ratiometric and colorimetric fluorescent probe for hypochlorite monitor and application for bioimaging in living cells, bacteria and zebrafish, J. Hazard. Mater. 388 (2020) Article Number 122029.
[10] Y.K. Yue, F.J. Huo, C.X. Yin, J.O. Escobedo, R.M. Strongin, Recent progress in chromogenic and fluorogenic chemosensors for hypochlorous acid, Analyst 141 (2016) 1859–1873.
[11] R. Scherz-Shouval, Z. Elazar, Regulation of autophagy by ROS: physiology and pathology, Trends Biochem. Sci. 36 (2011) 30–38.
[12] M. Schieber, N.S. Chandel, ROS function in redox signaling and oxidative stress 24 (2014) R453–R462.
[13] H.B. Xiao, X. Liu, C.C. Wu, Y.H. Wu, P. Li, X.M. Guo, B. Tang, A new endoplasmic reticulum-targeted two-photon fluorescent probe for imaging of superoxide anion in diabetic mice, Biosens. Bioelectron. 91 (2017) 449–455.
[14] K.Y. Liu, H.M. Shang, X.Q. Kong, M.G. Ren, J.Y. Wang, Y. Liu, W.Y. Lin, A novel near-infrared fluorescent probe for H_2O_2 in alkaline environment and the application for H_2O_2 imaging in vitro and in vivo, Biomaterials 100 (2016) 162–171.
[15] X.Q. Chen, X.Z. Tian, I. Shin, J. Yoon, Fluorescent and luminescent probes for detection of reactive oxygen and nitrogen species, Chem. Soc. Rev. 40 (2011) 4783–4804.
[16] H. Zhu, J.L. Fan, J.Y. Wang, H.Y. Mu, X.J. Peng, An "enhanced PET"-based fluorescent probe with ultrasensitivity for imaging basal and Elesclomol-induced HClO in cancer cells, J. Am. Chem. Soc. 136 (2014) 12820–12823.
[17] A. Strzepa, K.A. Pritchard, B.N. Dittel, Myeloperoxidase: a new player in autoimmunity, Cell. Immunol. 317 (2017) 1–8.
[18] M. Suwalsky, P. Orellana, M. Avello, F. Villena, Protective effect of Ugni molinae Turcz against oxidative damage of human erythrocytes, Food Chem. Toxicol. 45 (2007) 130–135.
[19] Z.Q. Mao, M.T. Ye, W. Hu, X.X. Ye, Y.Y. Wang, H.J. Zhang, C.Y. Li, Z.H. Liu, Design of a ratiometric two-photon probe for imaging of hypochlorous acid (HClO) in wounded tissues, Chem. Sci. 9 (2018) 6035–6040.
[20] Y.B. Wang, B.X. Zhao, Recent progress in fluorescent probes for the detection of hypochlorous acid, Chinese J. Org. Chem. 36 (2016) 1539–1554.

[21] N.J. Kruger, M.A. Troncoso-Ponce, R.G. Ratcliffe, ^{1}H NMR metabolite fingerprinting and metabolomic analysis of perchloric acid extracts from plant tissues, Nat. Protoc. 3 (2008) 1001–1012.
[22] M.G. Ren, K. Zhou, L.W. He, W.Y. Lin, Mitochondria and lysosome-targetable fluorescent probes for HOCl: recent advances and perspectives, J. Mater. Chem. B 6 (2018) 1716–1733.
[23] D.Q. Zhang, Highly selective and sensitive colorimetric probes for hypochlorite anion based on azo derivatives, Spectrochim. Acta A 77 (2010) 397–401.
[24] H.D. Li, J.L. Fan, X.J. Peng, Fluorescent probes for the recognition of hypochlorous acid, Prog. Chem. 29 (2017) 17–35.
[25] G. Li, D.D. Ji, S.M. Zhang, J.M. Li, C. Li, R.Z. Qiao, A mitochondria-targeting fluorescence turn-on probe for hypochlorite and its applications for *in vivo* imaging, Sensor Actuat. B-Chem. 252 (2017) 127–133.
[26] X. Wang, Y.M. Zhou, C.G. Xu, H.H. Song, L. Li, J.L. Zhang, M.X. Guo, A highly selective fluorescent probe for the detection of hypochlorous acid in tap water and living cells, Spectrochim. Acta A 203 (2018) 415–420.
[27] J. Han, Y.Y. Li, Y. Wang, X. Bao, L. Wang, L. Ren, L. Ni, C. Li, A water-soluble fluorescent probe for monitoring hypochlorite in water and in living cells, Sensor Actuat. B-Chem. 273 (2018) 778–783.
[28] L.D. Chen, H.L. Ding, N. Wang, Y. An, C.W. Lv, Two highly selective and sensitive fluorescent probes design and apply to specific detection of hypochlorite, Dyes Pigments 161 (2019) 510–518.
[29] C. Xu, Y. Qian, The α, β-unsaturated pyrazolone-based fluorescent sensor with red emission and its application for real-time monitoring hypochlorite in cancer cells and zebrafish, Dyes Pigments 161 (2019) 303–312.
[30] S. Jantra, P. Butta, P. Jithavech, P. Rojsitthisak, T. Palaga, P. Rashatasakhon, M. Sukwattanasinitt, S. Wacharasindhu, "Turn on" orange fluorescent probe based on styryl-BODIPY for detection of hypochlorite and its application in live cell imaging, Dyes Pigments 162 (2019) 189–195.
[31] H.H. Song, Y.M. Zhou, C.G. Xu, X. Wang, J.L. Zhang, Y. Wang, X.Q. Liu, M.X. Guo, X.J. Peng, A dual-function fluorescent probe: sensitive detection of water content in commercial products and rapid detection of hypochlorite with a large Stokes shift, Dyes Pigments 162 (2019) 160–167.
[32] Z.L. Wang, Y. Zhang, J. Song, M.X. Li, Y.Q. Yang, X. Xu, H.J. Xu, S.F. Wang, Three novel camphor-based fluorescence probes for ratiometric detection of hypochlorite and bio-imaging in living cells, Sensor Actuat. B-Chem. 284 (2019) 148–158.
[33] Z.W. Ma, X. Wang, C.C. Wang, X.P. Chen, Q.J. Lv, A sensitive and selective fluorescence probe for detection of hypochlorite (OCl^-) and its bioimaging in live cells, Spectrochim. Acta A 213 (2019) 370–374.
[34] E. Ahmmed, S. Lohar, S. Ghatak, S.K. Hira, P.P. Manna, P. Chattopadhyay, Development of a selective reaction-based turn-on fluorosensor and biomarker for hypochlorite ions in aqueous media, Anal. Methods 11 (2019) 2415–2421.
[35] H. Feng, Y. Wang, J.P. Liu, Z.Q. Zhang, X.Y. Yang, R. Chen, Q.T. Meng, R. Zhang, A highly specific fluorescent probe for rapid detection of hypochlorous acid in vivo and in water samples, J. Mater. Chem. B 7 (2019) 3909–3916.
[36] J.P. Gu, X.Q. Li, Z. Zhou, R.S. Liao, J.W. Gao, Y.P. Tang, Q.M. Wang, Synergistic regulation of effective detection for hypochlorite based on a dual-mode probe by employing aggregation induced emission (AIE) and intramolecular charge transfer (ICT) effects, Chem. Eng. J. 368 (2019) 157–164.
[37] X. Tang, Z. Zhu, R.J. Liu, Y. Tang, A novel ratiometric and colorimetric fluorescent probe for hypochlorite based on cyanobiphenyl and its applications, Spectrochim. Acta A 219 (2019) 576–581.
[38] X.X. Tang, H. Sun, J. Nie, X.E. Han, Y. Zhao, R. Zhang, Z.H. Ni, An o-hydroxyl aldehyde structure based naphthalimide derivative: reversible photochromic properties and its application in ClO^- detection in living cells, Spectrochim. Acta A 219 (2019) 154–163.
[39] Y. Jin, M.H. Lv, Y.F. Tao, S. Xu, J.L. He, J. Zhang, W.L. Zhao, A water-soluble BODIPY-based fluorescent probe for rapid and selective detection of hypochlorous acid in living cells, Spectrochim. Acta A 219 (2019) 569–573.
[40] W. Wang, J.Y. Ning, J.T. Liu, J.Y. Miao, B.X. Zhao, A mitochondria-targeted ratiometric fluorescence sensor for the detection of hypochlorite in living cells, Dyes Pigments 171 (2019) Article Number 107708.
[41] Z. Lu, M.Q. Shangguan, X.Z. Jiang, P.Y. Xu, L.X. Hou, T. Wang, A water-soluble cyclometalated iridium(III) complex with fluorescent sensing capability for hypochlorite, Dyes Pigments 171 (2019) Article Number 107715.
[42] Y.M. Zhang, H. Fang, W. Zhu, J.X. He, H. Yao, T.B. Wei, Q. Lin, W.J. Qu, Ratiometric fluorescent sensor based oxazolo-phenazine derivatives for detect hypochlorite via oxidation reaction and its application in environmental samples, Dyes Pigments 172 (2020) Article Number 107765.
[43] S. Malkondu, S. Erdemir, S. Karakurt, Red and blue emitting fluorescent probe for cyanide and hypochlorite ions: Biological sensing and environmental analysis, Dyes Pigments 174 (2020) Article Number 108019.
[44] S.L. Yi, Z. Lu, Y.D. Lin, J. Wang, Z.W. Qiao, R.K. Shen, J. Zhang, L.X. Hou, A novel mitochondria-targeted phosphorescence probe for hypochlorite ions detection in living cells, Talanta, 209 (2020) Article Number 120516.
[45] E. Rodrigo, I. Alonso, M.B. Cid, A protocol to transform sulfones into nitrones and aldehydes, Org. Lett. 20 (2018) 5789–5793.